Caution with Spectroscopic NO_2 Reference Cells (Cuvettes)

Ulrich Platt[1,2], Jonas Kuhn[1,2]

5

[1]Institute of Environmental Physics (IUP), Heidelberg University, INF 229,
D-69120 Heidelberg, Germany
[2]Max Planck Institute for Chemistry, Mainz, Germany

10   *Correspondence to:* Ulrich Platt (Ulrich.platt@iup.uni-heidelberg.de)

Abstract: Spectroscopic measurements of atmospheric trace gases, e.g. by Differential Optical Absorption Spectroscopy (DOAS) are frequently supported by recording the trace gas column density (CD) in absorption cells (cuvettes), which are temporarily inserted into the light-path.
15   The idea is to verify the proper working of the instruments, to check the spectral registration (wavelength calibration and spectral resolution), and to perform some kind of calibration (absolute determination of trace gas CDs). In principle DOAS applications do not require absorption cell calibration, however in practice measurements with absorption cells in the spectrometer's light path are frequently performed. In addition, trace gas absorption cells are
20   used as a central component in gas correlation spectroscopy instruments.
Here we show at the example of NO_2 absorption cells that the effective CD seen by the instrument can deviate greatly from expected values (by orders of magnitude). Analytical calculations and kinetic model studies show the dominating influence of photolysis and dimerisation of NO_2. In particular, this means that the partial pressure of NO_2 in the cell matters.
25   However, problems can be particular severe at high NO_2 pressures (around 10^5 Pa) as well as low NO_2 partial pressures (of the order of a few 100 Pa). Also, it can be of importance whether the cell contains pure NO_2 or is topped up with air or oxygen (O_2). Some suggestions to improve the situation are discussed.

1. INTRODUCTION

30

There are a number of reasons to use absorption cells in conjunction with instruments measuring trace gas column densities (CDs) by absorption spectroscopy, e.g. by Differential Optical Absorption Spectroscopy (DOAS). These include the verification of the overall working of the instrument, stray-light determination, or even a check of the instrument's absolute calibration
35   (which, however is inherent in DOAS and thus not needed, see e.g. Platt and Stutz, 2008).
In addition, gas correlation spectroscopy measurements (e.g. Ward and Zwick, 1975; Sandsten et al., 1996, 2004; Kebabian et al., 2000) require absorption cells containing the gas to be measured at CDs leading to optical densities around unity.
In general, there are a number of issues with using gas cells for these purposes including:
40   • Stability of the gas in the cell due to photolysis and/or chemical reactions
• Temperature dependence of chemical equilibria within the cell
• Temperature dependence of the optical density
• Optical problems with the cell
In the following we discuss the above problems for the case of NO_2 absorption cells, however
45   some of the discussed issues will also apply to cells with other gases.

Atmospheric
Measurement
Techniques
Discussions

2. OPTICS OF CELLS

In principle the introduction of an absorption cell into the optical path of a remote sensing instrument (e.g. a spectrometer) is straightforward. The cell is mounted in front of the entrance optics and in first approximation the absorption due to the trace gas in the cell (i.e. due to the trace gas CD) is added to the trace gas absorption seen without the cell. While this view is correct in some approximation, in detail there are a number of problems that need investigation.

2.1. Path length in an isolated cell

In a realistic cell partial reflection (reflectance R) occurs at the cell windows. For simplicity we assume an index of refraction of n=1.5 for the cell window material and accordingly

$$R = \left(\frac{n-1}{n+1} \right)^2 \approx 0.04 \qquad (1)$$

i.e. about 4% reflection per surface for near-normal incidence (see Fig. 1). While the reduction of the incoming intensity by $(1-R)^4$ or about 15% is probably of minor importance a fraction of about $(1-R)^2 \cdot (R+R)^2 \approx 0.59\%$ of the incoming radiation and 0.69% of the transmitted radiation passes the cell three times. Due to this multiple reflected light the total absorption of the cell (and thus the trace gas slant column density, SCD, S_C) will be enhanced by about 2%. We note the case of nearly normal incidence is quite realistic in many cases, for instance MAX-DOAS instruments (e.g. Hönninger and Platt, 2002, Platt and Stutz, 2008) have total aperture angles of the order of $1°$, i.e. incidence angles of -0.5° to +0.5°. A typical use of a cell would be to just mount it in front of the telescope. In this arrangement the enhancement of the light path inside the cell (and thus the trace gas column density S_C) due to the finite aperture angle of the radiation passing the cell will vary according to $S_C = S_0/\cos(\vartheta)$ with S_0 denoting the trace gas CD for rays parallel to the cell axis. An angle of $\vartheta = 0.5°$ would lead to an enhancement in S_C/S_0 of ≈ 1.000038 or 0.004%.
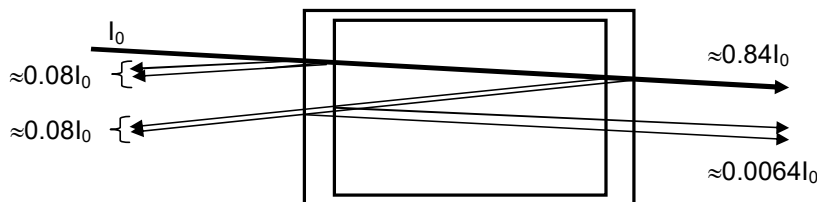

Fig. 1: Sketch of the optics of a gas absorption cell, parallel rays are assumed, the (small) tilt of the incoming ray with respect to the cell axis is introduced to distinguish the rays. The described effect will also be there at strictly normal incidence. We assume an index of refraction of n=1.5 for the cell window material and accordingly 4% reflection per surface (for near-normal incidence). Note that a fraction of about 0.69% of the transmitted radiation passes the cell three times thus adding $\approx 2\%$ to the total absorption.

Thus a slight (few degrees) tilt of the cell will not lead to noticeable light path extension in the cell, but already a 1° tilt, leading to 0.015% light path extension would be sufficient to reflect the multiple reflected light outside the field of view of the telescope. Thus, the additional 2% cell absorption would disappear. On the other hand, larger tilts of the cell, e.g. 10° would increase the cell absorption again by 1.5% and should therefore be avoided. This could be accomplished by a

Atmospheric
Measurement
Techniques
Discussions

rigid mount which fixes the (removable) cell at a defined angle with respect to the cell optical axis (normal of the windows), e.g. at 2°.

5   As will be discussed below, the acceptance angle oft the cell to ambient (sun)light can play a significant role. Therefore, this small aperture angle allows for shielding the cell from sunlight, since solar radiation does only need to enter from a small solid angle (of the order of 10^{-3} sr). This could be accomplished by mounting the cell inside a relatively long tube made of nontransparent material.

10   ## 2.2. Path length in a cell as part of an optical system

In section 2.1 we discussed the behaviour of an isolated cell, however the idea is to incorporate an absorption cell into an optical system, i.e. to just hold it in front of a MAX-DOAS instrument. In this case there can be interaction between the cell and the entrance optics of the instrument (for instance due to reflection of light at the surface of the telescope lens). As described by
15   Lübcke et al., (2013) this can further enhance the trace gas CD in the cell as seen by the instrument looking through it.

In the case of using gas cells gas in imaging instruments, for instance imaging spectrometers (e.g. Lohberger et al., 2004) or gas correlation instruments (e.g. Ward and Zwick, 1975) a larger aperture angle is required, which causes two potential problems: First, the aperture angle of the
20   cell has to be much larger than in the case of a one pixel (narrow field of view) instrument, for instance typically 30° total angle, thus the acceptance angle for solar radiation becomes considerably larger (e.g. 0.22 sr instead of 10^{-3} sr) and consequently the photolysis frequencies for the gases inside the cell (see below). Second, the trace gas CD of the cell becomes dependent on the observation angle ϑ (angle between the optical axis and the actual viewing direction
25   within the field of view), as described above. For a total aperture angle of 30° this would amount to an enhancement of the $S_C(15^o)$ over $S_0=S_C(0^o)$ of about 3.5%.

3.   CHEMISTRY IN NO_2-ABSORPTION CELLS

Nitrogen dioxide (NO_2) is a quite reactive gas, therefore a series of chemical processes in an
30   absorption cell can occur. Since they can alter the NO_2 concentration - and thus the NO_2 CD in the cell - considerably they have to be watched. In the following subsections we discuss the relevant chemical processes, starting with important reactions and then proceeding to further reactions, which are only relevant under certain conditions or if high precision is required.

3.1. The (initial) NO_2-only Chemistry – simple case

35   In a cell (initially) filled only with NO_2 we can expect the following reactions (bi-molecular rate constants are given in $cm^3 molec^{-1} s^{-1}$, termolecular rate constants are given in $cm^6 molec^{-2} s^{-1}$ for 25^oC and 1000 hPa, details on temperature and pressure dependence as well as literature references can be found in Table 1):

40   Usually cells are exposed to sun light or radiation needed for the measurement, thus NO_2 in the cell can be photolyzed:

$$NO_2 + h\nu \quad \rightarrow \quad NO + O(^3P) \quad J_1 \approx 8 \cdot 10^{-3} \text{ s}^{-1} \tag{R1}$$
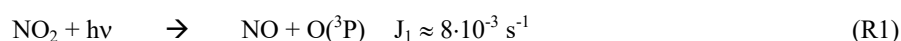
In the following ground state oxygen atoms $O(^3P)$ will be denoted by O. The threshold wavelength for reaction 1 is about 400 nm (e.g. Johnston and Graham, 1974, Burkholder et al.,
45   2015), however, due to vibrational excitation of the ground state molecule there is noticeable

Atmospheric
Measurement
Techniques
Open Access
Discussions

photolysis up to about 425 nm. If the cell is only illuminated with radiation of wavelength longer than 425 nm, NO_2 will not photolyze and J_1 will be essentially zero.

Although it is only a small effect it is worth noting that the photolysis frequency inside a cell is not different from the value in the air surrounding the cell as, despite reflectance of the cell walls as described by e.g. Bahe et al., 1979

The oxygen atoms produced in Reaction 1 can (1) recombine

$$O + O + M \quad \rightarrow \quad O_2 + M \tag{R2}$$

However, this is a slow process.

Alternatively, (2), O-atoms may react with the wall where they predominantly recombine (see e.g. Cartry et al., 2000):

$$O + O \qquad \rightarrow Wall \rightarrow \quad O_2 \tag{R3}$$

Also, (3) O-atoms can react with NO_2 to form NO:

$$O + NO_2 \quad \rightarrow \quad NO + O_2 \qquad k_4(298K) \approx 2.52 \cdot 10^{-12} \, cm^3 \, molec^{-1} \, s^{-1} \tag{R4}$$
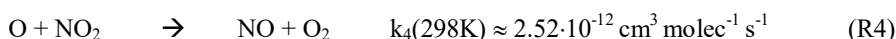
Further, (4), oxygen atoms also may react with NO to form NO_2:

$$O + NO + M \quad \rightarrow \quad NO_2 + M \qquad k_5(298K) \approx 2.2 \cdot 10^{-12} \, cm^3 \, molec^{-1} \, s^{-1} \tag{R5}$$
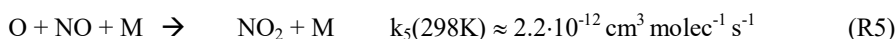
The final possibility (5) formation of NO_3 - as well as further reactions - will be treated in section 3.4, below.

In addition there is the termolecular reaction of the O_2 formed in reaction 4 (or added to the cell filling) oxidises NO to NO_2:

$$2\,NO + O_2 \quad \rightarrow \quad 2\,NO_2 \qquad k_6 \approx 1.95 \cdot 10^{-38} \tag{R6}$$
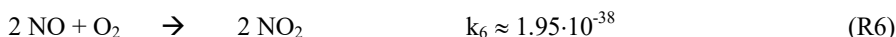
In an attempt to obtain a first order quantitative understanding of the processes in the cell we just consider a pure NO_2 initial filling and Reactions 1 (NO_2 photolysis), 4 ($O+NO_2$) and 6 ($2NO+O_2$):

From the combination of reactions 1 and 4 we derive the rates of NO and O_2 formation under illumination:

$$P(NO) = \frac{d}{dt}[NO] \approx 2 \cdot P(O_2) \approx 2 \cdot [NO_2] \cdot J_1 \tag{2}$$

Which ultimately (i.e. in the stationary state) must equal the rate of NO destruction, D(NO) and NO_2 formation, $P(NO_2)$ due to reaction 6:

$$D(NO) = -\frac{d}{dt}[NO] \approx P(NO_2) \approx 2 \cdot [NO]_S^2 \cdot [O_2] \cdot k_6 \tag{3}$$

Since $P(O_2) \approx 0.5 \cdot P(NO)$ and the concentration of both species are zero initially we have $[NO] \approx 2 \cdot [O_2]$. Substituting this relationship

$$D(NO) = -\frac{d}{dt}[NO] \approx [NO]^3 \cdot k_6 \tag{4}$$

and equating P(NO) with D(NO) we obtain:

$$2[NO_2] \cdot J_1 \approx [NO]_S^3 \cdot k_6 \tag{5}$$

Further substituting $[NO_2] \approx [NO_2]_0 - [NO]_S$:

Atmospheric
Measurement
Techniques
Discussions

$$[NO_2]_0 - [NO]_S \approx [NO]_S^3 \cdot \frac{k_6}{2J_1} \qquad (6)$$

or

$$[NO_2]_0 \approx [NO]_S^3 \cdot \frac{k_6}{2J_1} + [NO]_S \qquad (7)$$

This cubic equation can be solved for the stationary state NO concentration $[NO]_S$ as function of the initial $[NO_2]_0$ as given in Appendix 1.

Examples:

1) As an example and to obtain a first idea of what might be happening in the cell we assume about 1 atmosphere (1000 hPa) of pure NO_2 (initially) i.e. the initial NO_2 concentrations in the cell will be $[NO_2]_0 \approx 2.4 \cdot 10^{19}$ cm^{-3} and the very simple chemical system just comprising reactions 1, 4, and 6. As we shall show below the simplified reaction system - with the exception of the NO_2 dimer (N_2O_4) formation (see section 3.2) - is quite adequate. Also, such a cell would have a peak optical density (at around 440 nm) of about 14 at 1 cm length but much lower at other wavelengths.

In the dark ($J_1 = 0$) nothing will happen while in sun light ($J_1 = 8 \cdot 10^{-3}$): NO + O – formation will take place followed by reaction (4) of NO_2 with O. Thus the (initial) rate of NO formation P(NO) will be:

$$P(NO) \approx 2[NO_2]_0 \cdot J_1 \approx 3.8 \cdot 10^{17} cm^{-3}s^{-1} \qquad (8)$$

This will lead to an initial decay time $\tau_{NO2} = [NO_2]_0/P(NO) = 1/(2J_1) \approx 63$ s. The stationary state NO concentration can be calculated according to Equation 7 and the solution given in Appendix 1 to be $[NO]_S \approx 2.57 \cdot 10^{18}$ $molec/cm^3$ or about 10.7 % of the initial NO_2 level. In other words, the NO_2 concentration will be reduced to 89.3 % of its initial value $[NO_2]_0$. The corresponding NO rate of destruction will be:

$$D(NO) \approx [NO]^3 \cdot k_6 \approx 3.32 \cdot 10^{17} \, molec. \cdot cm^{-3}s^{-1}$$

matching $P(NO) \approx 2[NO_2]_S \cdot J_1$ from NO_2 photolysis .

2) We like to give a further example using about 1 hPa of pure NO_2 (initially) corresponding to $[NO_2]_0 \approx 2.4 \cdot 10^{16}$ cm^{-3}, and the same simple chemical system just comprising reactions 1, 4, and 6 as above. Such a cell would have an initial differential optical density in the vicinity of 450 nm of about $2.4 \cdot 10^{-3}$ and would thus appear ideal to test the sensitivity of a NO_2 spectrometer.

In sunlight we have $D(NO_2) \approx 1.92 \cdot 10^{14}$ $cm^{-3}s^{-1}$. In this case (using the same calculation as given in appendix 1) the resulting stationary state NO level becomes $[NO]_S \approx 2.4 \cdot 10^{16}$ or about 100% of the initial NO_2. In other words after illumination the remaining NO_2 concentration and thus the NO_2 CD of the cell will only be a very small fraction of the expected value ($[NO_2]_S \cdot J_1 = D(NO)$ or $[NO_2]_S = D(NO)/ J_1 \approx 1.7 \cdot 10^{13} cm^{-3}$ i.e. <0.1% of the initial $[NO_2]$). In other words, after a short (of the order of one minute) exposure to sunlight the NO_2 in the cell will practically vanish.

On the other hand, the NO re-conversion, D(NO), to NO_2 will be much slower than the initial photolysis:

$$D(NO) \approx 0.5 \cdot [NO]^3 \cdot k_6 \approx 1.35 \cdot 10^{11} \, molec. \cdot cm^{-3}s^{-1}$$

Recovery from illumination:
A further interesting question concerns the time for the chemical system to recover from a period of photolysis. Equation 4, gives the rate of NO destruction as function of [NO]. In the case of

example 1), above NO would decay with an initial rate of D(NO)/[NO]≈0.11/s (ca. 11% per second suggesting a 9 seconds time constant for recovery). However, D(NO) varies with the third power of [NO]. When e.g. 90% the NO is consumed (i.e. still 1.4% of [NO] is left) the time constant would increase by a factor of 1000 to around three hours.
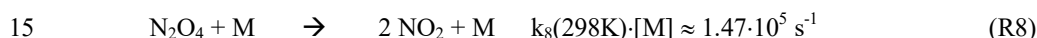
5   In the case of example 2) the initial re-conversion rate would only be $5.6 \cdot 10^{-6}$/s (or $\approx$ 49 % per day), which would seem to imply a recovery time of somewhat more than 2 days. But again the dependence on the cube of the NO concentration means that the recovery time becomes much longer later on. For some model results see Figure 7.

10   **3.2. The $NO_2 \leftrightarrow N_2O_4$ Equilibrium·**

An additional problem in NO_2 cells - in particular if high NO_2 concentrations approaching 1000 hPa are used - is the formation of the dimer N_2O_4 (see also Roscoe et al. 1993):

$$2\ NO_2 + M \quad \rightarrow \quad N_2O_4 + M \qquad k(298K)\cdot[M] \approx 3.3\cdot10^{-14}\ cm^3\ molec^{-1}\ s^{-1} \qquad (R7)$$
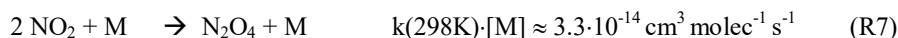
There is a thermal decay of the dimer:

15    $$N_2O_4 + M \quad \rightarrow \quad 2\ NO_2 + M \qquad k_8(298K)\cdot[M] \approx 1.47\cdot10^5\ s^{-1} \qquad (R8)$$

Leading to an equilibrium with the equilibrium constant (298K, from Atkinson et al. 2014):

$$K_{Eq} = \frac{k_{\rightarrow}}{k_{\leftarrow}} = \frac{[N_2O_4]}{[NO_2]^2} \approx 2.29\cdot10^{-19}\ cm^3\ molec^{-1} \qquad (9)$$

Note that the time to attain the equilibrium is shorter than $1/k_8 \approx 7\ \mu s$ (at 298 K and 1000 hPa) thus one can assume that there is always equilibrium between NO_2 and N_2O_4. From this follows

20   for the $[NO_2]/[N_2O_4]$ ratio:

$$\frac{1}{K_{Eq}[NO_2]} = \frac{[NO_2]}{[N_2O_4]} \quad or \quad [N_2O_4] = K_{Eq} \cdot [NO_2]^2 \qquad (10)$$

What is usually most interesting is the fraction of NO_2 of the total amount of $NO_2+N_2O_4$ (i.e. pressure during filling) in the cell. The latter is given by $[NO]_Z = [NO_2]+[N_2O_4]$ and thus:

$$\frac{[NO_2]}{[NO_2]_Z} = \frac{[NO_2]}{[N_2O_4]+[NO_2]} = \frac{[NO_2]}{K_{Eq} \cdot [NO_2]^2 + [NO_2]} = \frac{1}{K_{Eq} \cdot [NO_2]+1} \qquad (11)$$

25   Which can be transformed to:

$$K_{Eq} \cdot [NO_2]+1 = \frac{[NO_2]_Z}{[NO_2]} \Rightarrow [NO_2]_Z = K_{Eq} \cdot [NO_2]^2 + [NO_2] \qquad (12)$$

And solved for $[NO_2]$:

$$[NO_2]^2 + \frac{[NO_2]}{K_{Eq}} - \frac{[NO_2]_Z}{K_{Eq}} = 0 \qquad (13)$$

With the only positive solution:

30    $$[NO_2]_1 = -\frac{1}{2K_{Eq}} + \sqrt{\frac{1}{4K_{Eq}^2} + \frac{[NO_2]_Z}{K_{Eq}}} \qquad (14)$$

or

Atmospheric
Measurement
Techniques
Discussions

$$\left[NO_2\right]_l = \frac{1}{K_{Eq}}\left(-\frac{1}{2}+\sqrt{\frac{1}{4}+\left[NO_2\right]_Z \cdot K_{Eq}}\right) \tag{15}$$

The relationship between NO_2 and $[NO_2]/[NO_Z]$ in the cell as a function of total $[NO]_Z = [NO_2]+[N_2O_4]$ is shown in Figure 2.

5 Examples: $[M]=2.4\cdot10^{19}$ (1000 hPa or ca. 1 atmosphere of total pressure, at 298 K) resulting in $[NO_2]_l \approx 8.29 \cdot 10^{18}$ molec/cm^3 and $[NO_2]_l/[NO]_Z \approx 0.344$. Thus, filling a cell from an NO_2 reservoir (e.g. an NO_2 tank) to one atmosphere of total pressure will lead to only 32% of this pressure being present as NO_2 (see also Figure 2).

At 100, 10, 1 hPa (ca. 0.1, 0.01, and 0.001 atmospheres) of $NO_2+N_2O_4$ the corresponding figures
10 for $[NO_2]_l/[NO]_Z$ would be 0.717, 0.95, and 0.99.5, respectively. These figures are independent of an additional topping with air or oxygen to a full atmosphere of total pressure, as will be described below. In other words unless the NO_2 partial pressure is around 100 Pa the actual NO_2 partial pressure (and thus concentration of NO_2) will be below expected levels by two-digit percentages.

15

A further problem associated with the $NO_2 - N_2O_4$ equilibrium is the marked temperature dependence of the equilibrium constant. In the usual Arrhenius expression it is given as:

$$K_{Eq}(T) = A \cdot e^{\frac{B}{T}} \tag{16}$$

With $A = 1.07 \cdot 10^{-28}$ cm^3/molec and $B = 6400$ K (see Table 1). The (relative) temperature
20 dependence of K_{Eq} is given by:

$$\frac{1}{K_{Eq}(T)}\frac{d}{dT}\left(K_{Eq}(T)\right) = \frac{1}{K_{Eq}(T)}A \cdot e^{\frac{B}{T}}\frac{d}{dT}\left(\frac{B}{T}\right) = \frac{1}{K_{Eq}(T)}\cdot-\frac{AB}{T^2}\cdot e^{\frac{B}{T}} = -\frac{B}{T^2} \tag{17}$$

With the above values for A and B we obtain for the relative change in the equilibrium constant:

$$\frac{1}{K_{Eq}(T)}\frac{d}{dT}\left(K_{Eq}(T)\right) = -\frac{B}{T^2} \approx -0.072\frac{1}{K} \tag{18}$$

In other words the equilibrium constant is reduced by more than 7%/K of heating. Fortunately
25 the effect on NO_2 is somewhat smaller, ranging from near zero change at very small NO_2 levels to about 3% increase per degree of heating at 1000 hPa (see section 4).
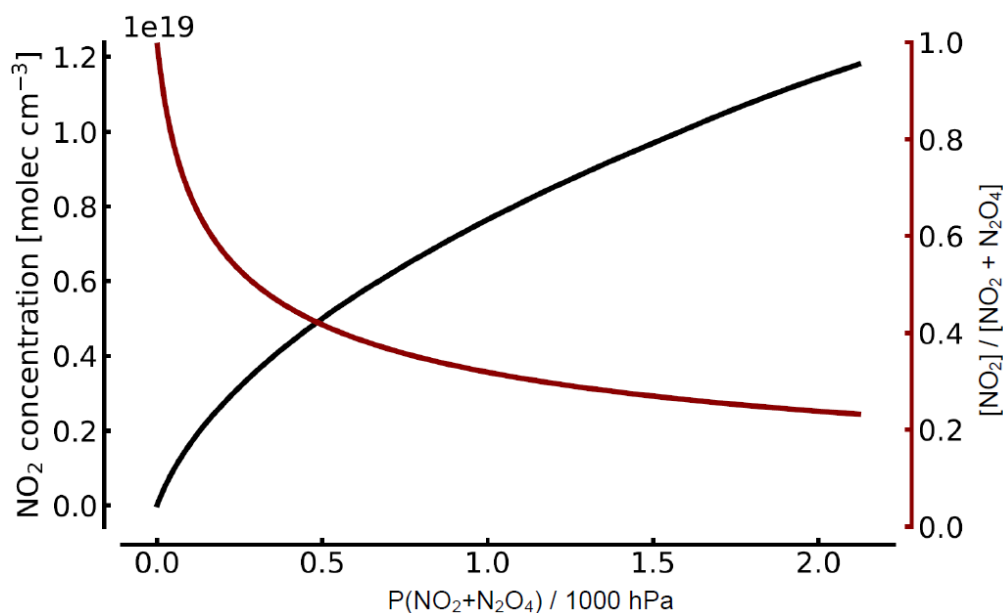
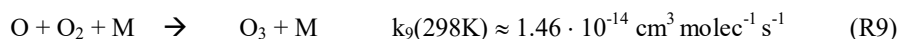*Fig. 2: NO_2-concentration (black line in units of 10^{19} molec/cm^2, left axis) and fraction of NO_2 (red line, right axis) of the total $[NO_2]_Z = [NO_2] + [N_2O_4]$ as a function of $[NO_2]_Z$ (given in pressure units for 25°C). At atmospheric pressure (1000 hPa) in the cell only about 34% of the total NO_{2Z} (or ≈ 344 hPa partial pressure) exist as NO_2.*
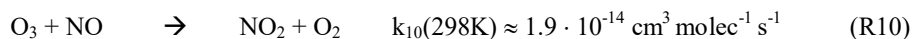
3.3. $NO_2 + O_2$ chemistry

The addition of O_2 (or air) to the NO_2 filling has two effects that can greatly help stabilising the NO_2 concentration in a cell under certain conditions, as explained below:

1) In the presence of molecular oxygen following the photolysis of NO_2 ozone is formed in the cell:

$$O + O_2 + M \quad \rightarrow \quad O_3 + M \qquad k_9(298K) \approx 1.46 \cdot 10^{-14} \text{ cm}^3 \text{ molec}^{-1} \text{ s}^{-1} \qquad (R9)$$

Which in turn can react with NO to form NO_2:

$$O_3 + NO \quad \rightarrow \quad NO_2 + O_2 \qquad k_{10}(298K) \approx 1.9 \cdot 10^{-14} \text{ cm}^3 \text{ molec}^{-1} \text{ s}^{-1} \qquad (R10)$$

The reaction scheme encompassing the pertinent reaction pathways discussed above is sketched in Figure 3.
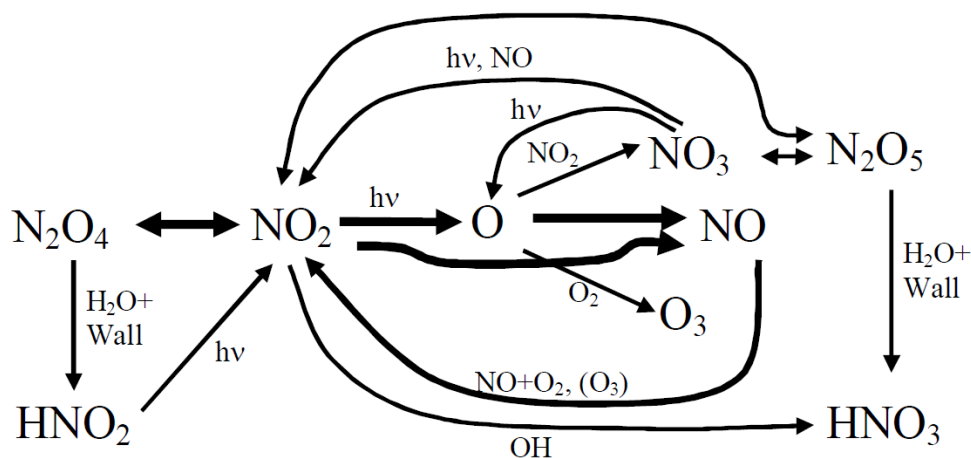
Fig. 3: Simplified scheme of the chemical reactions in an illuminated NO_2-cell. The reactions in the 'NO$_2$ only' system are indicated by fat arrows. Formation of OH is not shown.

5

Here we can distinguish two regimes:

a) Comparable concentrations of O_2 and NO_2 i.e. $[O_2]/[NO_2]$ around unity. In this case the termolecular oxidation of NO by O_2 dominates, this is similar to the situation discussed in section 3.1, however we can take the O_2 concentration $[O_2]$ to be essentially constant. This reduces the third order kinetics of Equation 7 to (pseudo) second order kinetics and we obtain:

$$[NO] = \sqrt{\frac{P_{NO}}{2[O_2]k_{NO}}} \underset{P_{NO}\text{ substituded}}{\approx} \sqrt{\frac{[NO_2]\cdot J}{[O_2]k_{NO}}}$$

(19)

$$\frac{[NO]}{[NO_2]} \approx \sqrt{\frac{J}{[O_2][NO_2]k_{NO}}}$$

For example we may assume 0.5 atmospheres (500 hPa), each of pure NO_2 and O_2 (initially) i.e. the initial concentrations of either species in the cell will be $[O_2]_0 = [NO_2]_0 \approx 1.2 \cdot 10^{19}$ cm^{-3}. In sunlight we have NO_2 photolysis (reaction 1) followed by $O+NO_2$ (reaction 4) plus oxidation of NO by O_2.

$$D(NO) \approx 2[NO]^2 \cdot [O_2]k_{NO} = P(NO)$$

From this stationary state assumption we can calculate $[NO]_s$:

$$[NO]_s \approx \sqrt{\frac{P_{NO}}{2[O_2]k_{NO}}} \approx 0.054 \cdot [NO_2]$$

20   Thus the NO_2 concentration would be reduced by only 5.4% from its initial value once the cell is subjected to sunlight.

Atmospheric
Measurement
Techniques
Discussions

b) High $[O_2]/[NO_2]$ ratio (for instance larger than 10^4), so that the reaction of O-atoms formed in NO_2 photolysis are much more likely to react with O_2 than with NO_2. In this case for each molecule of NO_2 photolyzed nearly one molecule of O_3 is formed, which will react with the NO molecule produced in the NO_2 photolysis. The O_3 concentration will rise until its reaction with NO balances the rate of NO_2 photolysis:
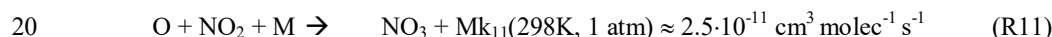
$$[NO][O_3]k_{10} = [NO_2] \cdot J_1 \tag{20}$$

Since $[NO] \approx [O_3]$ we obtain:

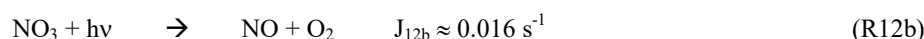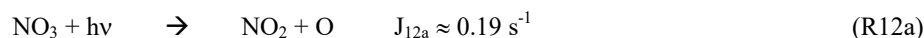$$[NO]^2 k_{10} \approx [NO_2] \cdot J \Rightarrow [NO] \approx \sqrt{\frac{[NO_2] \cdot J}{k_{10}}} \tag{21}$$

For instance at $[NO_2] = 2.4 \cdot 10^{15}$ cm^{-3} and about one atmosphere (1000 hPa) of O_2 the stationary state NO level would be $[NO] \approx 4.4 \cdot 10^{13}$ cm^{-3} or about 1.8% of the initial NO_2 concentration. Note that a small fraction (about 10^{-4} in this example) of the O-atoms produced in the NO_2-photolysis would still react with NO_2 and form NO without a corresponding O_3 production (rate about $2 \cdot 10^9$ cm^{-3}s^{-1}), thus the NO-fraction in the cell would slowly grow until reaction 6 balances this process. At the above NO level the rate of NO_2 formation would be around 10^9 cm^{-3}s^{-1}, thus the NO level would slightly grow (by about 50%) during several days of continuous illumination of the cell.

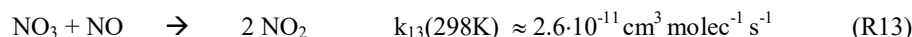### 3.4. The (initial) NO$_2$-only Chemistry – some complications

In addition to the three reactions described above, O-atoms can recombine with NO_2 to form nitrate radicals, NO_3:
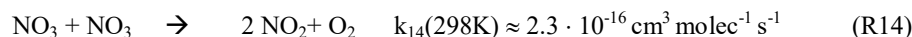
$$O + NO_2 + M \rightarrow \quad NO_3 + M \quad k_{11}(298K, 1 \text{ atm}) \approx 2.5 \cdot 10^{-11} \text{ cm}^3 \text{ molec}^{-1} \text{ s}^{-1} \tag{R11}$$

The thus formed NO_3 radicals can be photolyzed:

$$NO_3 + h\nu \quad \rightarrow \quad NO_2 + O \qquad J_{12a} \approx 0.19 \text{ s}^{-1} \tag{R12a}$$

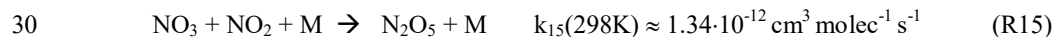$$NO_3 + h\nu \quad \rightarrow \quad NO + O_2 \qquad J_{12b} \approx 0.016 \text{ s}^{-1} \tag{R12b}$$

The threshold wavelength is much longer than in the case of NO_2 (J_1) and the photolysis is much faster. Alternatively, NO_3 may react with NO (from R1) to re-form NO_2:
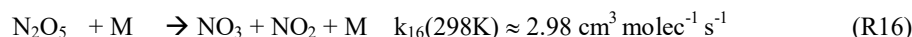
$$NO_3 + NO \quad \rightarrow \quad 2 NO_2 \qquad k_{13}(298K) \approx 2.6 \cdot 10^{-11} \text{ cm}^3 \text{ molec}^{-1} \text{ s}^{-1} \tag{R13}$$

Or undergo self reaction:

$$NO_3 + NO_3 \quad \rightarrow \quad 2 NO_2 + O_2 \qquad k_{14}(298K) \approx 2.3 \cdot 10^{-16} \text{ cm}^3 \text{ molec}^{-1} \text{ s}^{-1} \tag{R14}$$

Finally, and typically most likely, NO_3 will react with NO_2 to form dinitrogen pentoxide, N_2O_5:

$$NO_3 + NO_2 + M \rightarrow N_2O_5 + M \qquad k_{15}(298K) \approx 1.34 \cdot 10^{-12} \text{ cm}^3 \text{ molec}^{-1} \text{ s}^{-1} \tag{R15}$$

Dinitrogen pentoxide is thermally unstable and decays:

$$N_2O_5 + M \rightarrow NO_3 + NO_2 + M \quad k_{16}(298K) \approx 2.98 \text{ cm}^3 \text{ molec}^{-1} \text{ s}^{-1} \tag{R16}$$

In the absence of water (dry system) N_2O_5 will just be another reservoir potentially sequestering some of the NO_2. On the other hand, N_2O_5 is the anhydride of nitric acid and may react with water to form HNO_3. While the N_2O_5 plus water vapour reaction appears to be exceedingly slow it may react with a layer at the cell surface, details are given in section 3.5.

Analyzing the above system of reactions one notices that loss of O-atoms other than by reactions 4 or 11 are of minor importance. This is underlined by the results of the model calculations using the full chemical system (see Table 1) presented in section 4.
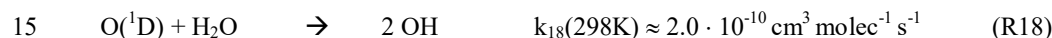
Atmospheric
Measurement
Techniques
Discussions

Open Access
EGU

Therefore, we can summarize that each photolysis reaction (R1) is followed by a conversion of NO_2 to NO (R4) or to NO_3 (R11). However, NO_3 is largely converted back to NO_2 by reactions 12a, 13, and (to a minor extent) 14, thus, in effect each photolysis act of NO_2 leads to the loss of approximately two NO_2 molecules. Essentially NO_2 would be converted to NO + O_2. In bright

5   sunshine with $J_1 \approx 8 \cdot 10^{-3}$ s^{-1} this would lead to a NO_2 – lifetime in the cell of $\tau(NO_2) \approx 1/(2 \cdot J_1) \approx 63$ s or roughly one minute. Even if the cell is kept in the shade or is only exposed to indoor illumination where J_1 could be estimated to be 10-times (shade) to 100-times (indoor) smaller than in bright sunshine the conversion could be expected to proceed within around 10 (shade) to 100 (indoor) minutes.
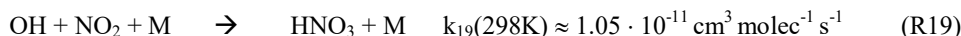
10   ### 3.5. NO_2 + O_2 + (trace) H_2O chemistry

It may be possible that traces of water enter the cell when it is filled, then a series of additional reactions may play a role:
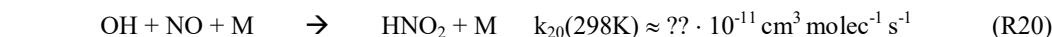
$$O_3 + h\nu \quad \rightarrow \quad O(^1D) + O_2 \quad J \approx 3 \cdot 10^{-5} \text{ s}^{-1} \tag{R17}$$
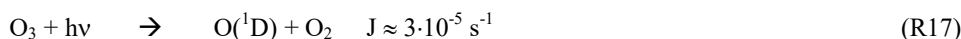
Followed by quenching of $O(^1D)$ to $O(^3P)$ or the formation of hydroxyl (OH) radicals:

15    $$O(^1D) + H_2O \quad \rightarrow \quad 2 \text{ OH} \quad k_{18}(298K) \approx 2.0 \cdot 10^{-10} \text{ cm}^3 \text{ molec}^{-1}\text{ s}^{-1} \tag{R18}$$

In an NO_2 cell OH radicals are most likely to react with NO_2 to form nitric acid:

$$OH + NO_2 + M \quad \rightarrow \quad HNO_3 + M \quad k_{19}(298K) \approx 1.05 \cdot 10^{-11} \text{ cm}^3 \text{ molec}^{-1}\text{ s}^{-1} \tag{R19}$$

Nitric acid is photolyzed very slowly, also its reaction with OH (to form NO_3) is slow, thus it will constitute a final sink of NO_2 (and water) in the cell. Alternatively OH may react with NO to

20   form nitrous acid:

$$OH + NO + M \quad \rightarrow \quad HNO_2 + M \quad k_{20}(298K) \approx ?? \cdot 10^{-11} \text{ cm}^3 \text{ molec}^{-1}\text{ s}^{-1} \tag{R20}$$

Which – in turn – is lost by photolysis:

$$HNO_2 + h\nu \quad \rightarrow \quad OH + NO \quad j_{21}(298K) \approx 1.34 \cdot 10^{-3} \text{ s}^{-1} \tag{R21}$$
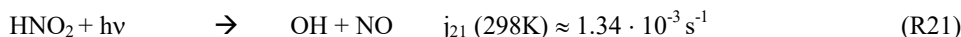
In addition N_2O_5, formed in reaction 15, can react with (liquid) water adsorbed at the wall of the

25   cell, also forming HNO_3:

$$N_2O_5 + (H_2O)_{liq} \quad \rightarrow \quad 2 \text{ } (HNO_3)_{liq} \tag{R22}$$
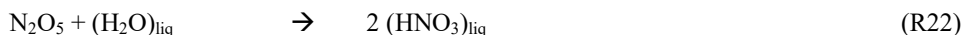
Finally N_2O_4 is also known to heterogeneously react with water:

$$N_2O_4 + (H_2O)_{liq} \quad \rightarrow \quad HNO_2 + (HNO_3)_{liq} \tag{R23}$$

HNO_2 will relatively quickly photolyze to form OH + NO (with OH in most cases reacting

30   according to R19), and HNO_3 from the above two reactions will remain. One can actually assume that all H_2O is ultimately converted to HNO_3, sequestering equivalent amounts of NO_2 and water.

For example a cell having been filled with a small amount of NO_2 (e.g. 10 hPa or

35    $2.4 \cdot 10^{17}$ molec cm^{-3}) is topped with laboratory air at 25°C and 70% relative humidity. Thus the approximate amount of water admitted is 70% of the saturation vapour pressure of H_2O at that temperature (70% of 31.6 hPa = 22.1 hPa or $5.3 \cdot 10^{17}$ molec cm^{-3}). Some of this water will form a film at the inside of the cell and allow heterogeneous reactions 22 and 23 converting NO_2 into HNO_3, although it is hard to judge how fast this process will proceed. In addition, upon

40   illumination with UV radiation reaction sequence 9, 17, 18, 19 will provide (relatively slow) gas-phase conversion of NO_2 to HNO_3. Since the amount of H_2O in this example exceeds the amount of NO_2 it is likely that ultimately all NO_2 is converted to HNO_3.

Table 1: Summary of reaction rate constants ([1]: data from Burkholder et al., 2015 (JPL Publication 15-10; [2]: data from Atkinson et al., 2004; [3]: data from Tsang and Hampson, 1986; [4]: data from Trebs et al., 2009, [5]: data from Bahe and Schurath, 1978, [6]: data from Alicke et al., 2002). The reactions marked with * are included in the kinetic model, see Section 4.

5

No.	Reaction	k(T), j, or k_0(T) $cm^3 molec^{-1} s^{-1}$ if not given otherwise	k_∞	k(298 K, 1 atm) or j $cm^3 molec^{-1} s^{-1}$ if not given otherwise
1*,[4]	$NO_2 + h\nu \rightarrow NO + O$	$8 \cdot 10^{-3}$ s^{-1}		$8 \cdot 10^{-3}$ s^{-1}
2*,[3]	$O + O + M \rightarrow O_2 + M$	$5.21 \cdot 10^{-35} e^{(900/T)}$ $cm^6 molec^{-2} s^{-1}$		$2.51 \cdot 10^{-14}$
3	$O + O \rightarrow Wall \rightarrow O_2$	neglected		
4*,[1]	$O + NO_2 \rightarrow NO + O_2$	$5.1 \cdot 10^{-12} \cdot e^{(-210/T)}$		$2.52 \cdot 10^{-12}$
5*,[1]	$O + NO + M \rightarrow NO_2 + M$	$9 \cdot 10^{-32}(T/300)^{-1.5}$ $cm^6 molec^{-2} s^{-1}$	$3.0 \cdot 10^{-11}$	$2.2 \cdot 10^{-12}$
6*,[2]	$2 NO + O_2 \rightarrow 2 NO_2$	$3.3 \cdot 10^{39}$ $exp(530/T)$ $cm^6 molec^{-2} s^{-1}$		$1.95 \cdot 10^{-38}$ $cm^6/(molec^2 s)$
7*,[2]	$2 NO_2 + M \rightarrow N_2O_4 + M$	$1.4 \cdot 10^{-33}(T/300)^{-3.8}$ $cm^6 molec^{-2} s^{-1}$	$1.0 \cdot 10^{-12}$	$3.3 \cdot 10^{-14}$
8*,[2]	$N_2O_4 + M \rightarrow 2 NO_2 + M$	$1.3 \cdot 10^{-5}(T/300)^{-3.8}$ $e^{(-6400/T)}$	$1.15 \cdot 10^{16} e^{(-6460/T)}$ s^{-1}	$1.47 \cdot 10^5$ s^{-1}
9*,[1]	$O + O_2 + M \rightarrow O_3 + M$	$6.0 \cdot 10^{-34}(T/300)^{-2.4}$ $cm^6 molec^{-2} s^{-1}$	$k_0[M] \ll k_\infty$ at 1000 hPa	$1.46 \cdot 10^{-14}$
10*,[1]	$O_3 + NO \rightarrow NO_2 + O_2$	$3.0 \cdot 10^{-12} e^{(1500/T)}$		$1.9 \cdot 10^{-14}$
11*,[1]	$O + NO_2 + M \rightarrow NO_3 + M$	$2.5 \cdot 10^{-31}(T/300)^{-1.8}$	$2.2 \cdot 10^{-11}$ $(T/300)^{-0.7}$	$6.1 \cdot 10^{-12}$
12a*,[2]	$NO_3 + h\nu \rightarrow NO_2 + O$	0.19 s^{-1}		0.19 s^{-1}
12b*,[2]	$NO_3 + h\nu \rightarrow NO + O_2$	0.016 s^{-1}		0.016 s^{-1}
13*,[1]	$NO_3 + NO \rightarrow 2 NO_2$	$1.5 \cdot 10^{-11} e^{(170/T)}$		$2.6 \cdot 10^{-11}$
14*,[1]	$NO_3 + NO_3 \rightarrow 2 NO_2 + O_2$	$8.5 \cdot 10^{-13} e^{(-2450/T)}$		$2.3 \cdot 10^{-16}$
15*,[1]	$NO_3 + NO_2 + M \rightarrow N_2O_5 + M$	$2.4 \cdot 10^{-30}(T/300)^{-3.0}$ $cm^6 molec^{-2} s^{-1}$	$1.6 \cdot 10^{-12}$ $(T/300)^{0.1}$	$1.34 \cdot 10^{-12}$
16*,[2]	$N_2O_5 + M \rightarrow NO_3 + NO_2 + M$	$1.3 \cdot 10^{-3}(T/300)^{-3.5}$ $e^{(-11000/T)}$ s^{-1}	$9.7 \cdot 10^{14}(T/300)^{0.1}$ $e^{(-11080/T)}$ s^{-1}	2.98 s^{-1}
17[5]	$O_3 + h\nu \rightarrow O(^1D) + O_2$	$3 \cdot 10^{-5}$ s^{-1}		$3 \cdot 10^{-5}$ s^{-1}
18[1]	$O(^1D) + H_2O \rightarrow 2 OH$	$1.63 \cdot 10^{-10} \cdot e^{(60/T)}$		$2.0 \cdot 10^{-10}$
19[1]	$OH + NO_2 + M \rightarrow HNO_3 + M$	$1.8 \cdot 10^{-30} (T/300)^{-3}$	$2.8 \cdot 10^{-11}$	$1.05 \cdot 10^{-11}$
20	$OH + NO + M \rightarrow HNO_2 + M$	$7 \cdot 10^{-31} (T/300)^{-2.6}$	$3.6 \cdot 10^{-11} (T/300)^{-0.1}$	$9.7 \cdot 10^{-12}$
21[6]	$HNO_2 + h\nu \rightarrow OH + NO$	$1.34 \cdot 10^{-3}$		
22	$N_2O_5 + (H_2O)_{liq} \rightarrow 2(HNO_3)_{liq}$	neglected		
23	$N_2O_4 + H_2O \rightarrow HNO_2 + HNO_3$	neglected		

Atmospheric
Measurement
Techniques
Discussions

Open Access

4. GAS KINETIC SIMULATIONS

A series of gas kinetic simulation calculations were performed in order to check on the simplified analytical calculations in the previous section.

5   In a one-box model, the system of coupled ordinary differential equations resulting from the above reactions was solved numerically. This allows to follow the temporal evolution of the concentration of the individual gases in the cell under given conditions. Our full model includes Reaction 1 to Reaction 16 of Table 1 (marked with an asterisk in column 1) and neglects possible wall losses (reaction 3). Also some runs with a subset of the reactions were performed as
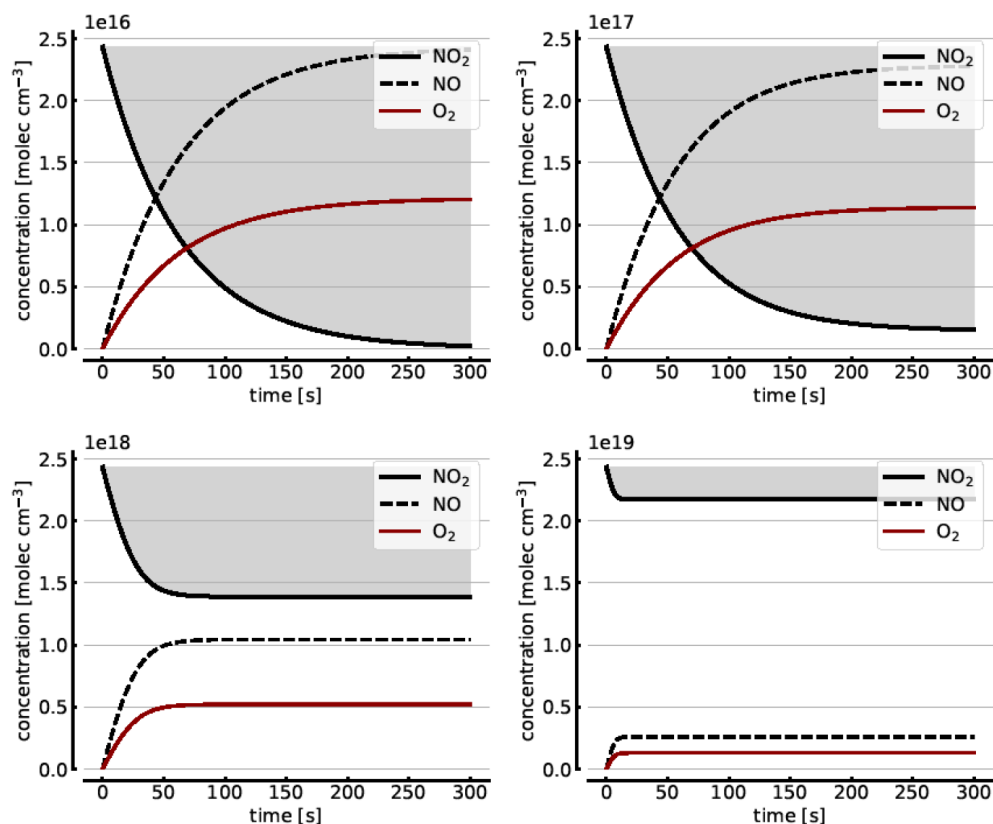10   described below.

The first reaction kinetic model calculations show the temporal evolution of $[NO_2]$, $[NO]$, $[O_2]$, according to the simple reaction system (reactions 1, 4, and 6) in an illuminated NO_2-cell. In particular we initially neglect the NO_2 dimer formation. These calculations merely serve to demonstrate that the analytical solution as derived in section 3.1 matches the model calculations.

15   Figure 4 shows some results of this (over)simplified model assuming (as above) initial NO_2 levels $[NO_2]_0$ of 1, 10, 100, 1000 hPa ($2.4 \cdot 10^{16}$, $2.4 \cdot 10^{17}$, $2.4 \cdot 10^{18}$, $2.4 \cdot 10^{19}$ molec/cm^3), respectively. As expected the initial NO_2 concentration drops within the first few seconds (at high initial NO_2) to minutes (at low NO_2) until the back-reaction kicks in and leads to stationary state levels of all species after this initial period. At 1 hPa initial NO_2 its concentration drops to
20   very small levels (< 0.1 %) as shown in section 3.1 while at 1000 hPa we still see about 10.7 % loss of initial NO_2 These figures are exactly the same as found from the steady state calculations (see Appendix 1).

Figure 5 shows some results of the simplified model (reactions 1, 4, and 6) but including the NO_2
25   - N_2O_4 equilibrium (reactions 7 and 8) for initial NO_2 levels, $[NO_2]_0$ of 1, 10, 71, 344 hPa ($2.4 \cdot 10^{16}$, $2.4 \cdot 10^{17}$, $1.7 \cdot 10^{18}$, $0.84 \cdot 10^{19}$ molec/cm^3, due to filling the cell with NO_2 levels of 1, 10, 100, 1000 hPa, which then immediately undergo N_2O_4 equilibration), respectively. For the lower initial NO_2 levels (1, 10 hPa) there is little difference to Figure 4: The initial NO_2 concentration drops within the first few seconds to minutes to small fractions of the initial $[NO_2]_0$. As
30   discussed above (Sect. 3.3), the situation can be improved by adding initial O_2 (topped up to 1000 hPa). The thin blue line in the plots for $[NO_2]_0 = 1, 10, 71$ hPa indicates the results for the corresponding NO_2 profiles. In particular at higher initial NO_2 levels (e.g. 71 hPa) the ultimate NO_2 levels are considerably enhanced by O_2 addition. However at higher initial NO_2 levels (see plots for 71 and 344 hPa initial NO_2) there is a large reduction in NO_2 due to the NO_2-dimer
35   formation inducing stronger temperature dependence.

In order to get a feeling for the influence of temperature changes in the model run for $[NO_2]_0 = 344$ hPa the temperature was raised by 5 K (298 K to 303 K) after 100s, the corresponding plot (bottom right in Fig. 5) shows an increase in NO_2 (thin blue line) of about 16% due to this temperature rise.

40

Fig. 4: Model calculations of the temporal evolution of [NO$_2$] (thick drawn black line), [NO] (dashed black line), [O$_2$] (drawn brown line) according to the simple reaction system (reactions 1, 4, and 6 only, at 298 K) in an illuminated NO$_2$-cell. Here the NO$_2$ - N$_2$O$_4$ chemical equilibrium is neglected, which makes in particular the plots for initial [NO$_2$]$_0$ = 1000 hPa unrealistic. All time series are for calculation with no added initial O$_2$. Initial [NO$_2$]$_0$ = 1, 10, 100, 1000 hPa (2.4·10^{16}, 2.4·10^{17}, 2.4·10^{18}, 2.4·10^{19} molec/cm^3), respectively.
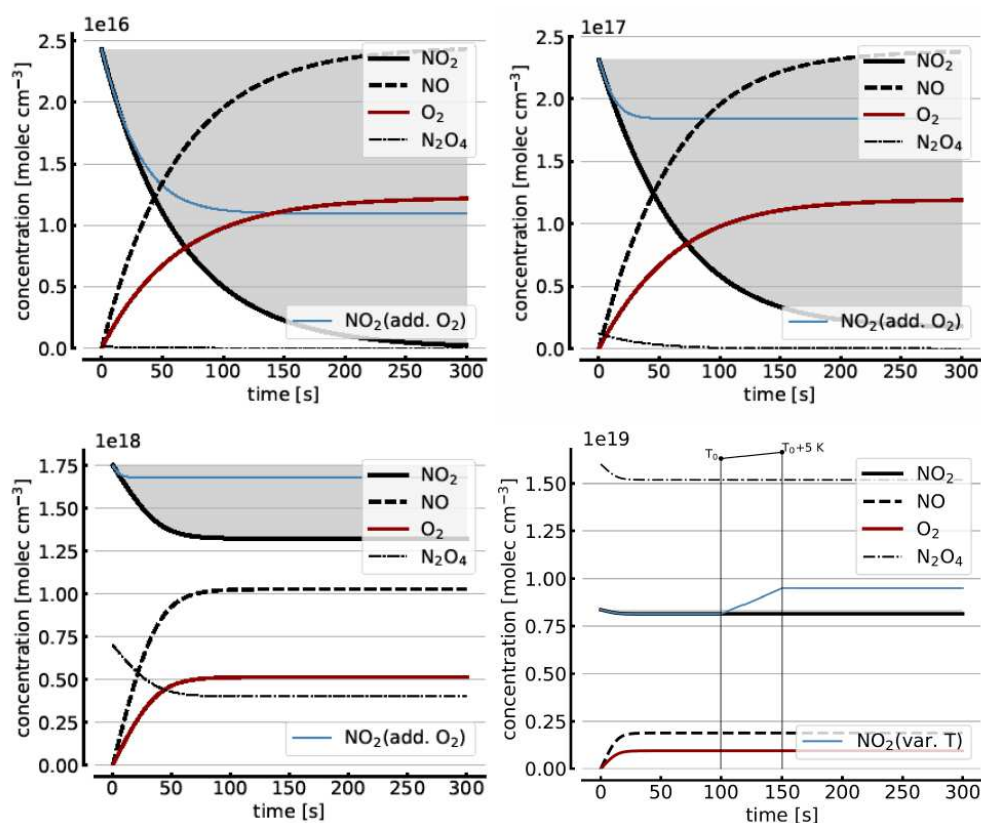
5

Fig. 5: *Same Model calculations as shown in Fig 4 but including N_2O_4. Initial $[NO_2]_0 = 1, 10,*
    71, 344 hPa ($2.4 \cdot 10^{16}$, $2.4 \cdot 10^{17}$, $1.7 \cdot 10^{18}$, $0.8 \cdot 10^{19}$ molec/cm^3), respectively, see text.
    Temporal evolution of $[NO_2]$ (thick drawn black line), $[NO]$ (dashed black line), $[O_2]$
5   *(drawn brown line), and $[N_2O_4]$ (thin dashed-dotted line) according to the simple reaction*
    system (reactions 1, 4, 6, 7, and 8 only, at 298 K) in an illuminated NO_2-cell. All time series
    with the exception of the thin blue line (in the plots for $[NO_2]_0 = 1, 10, 71$ hPa) are for
    calculation with no added initial O_2. The thin blue line (in the plots for $[NO_2]_0 = 1, 10, 71$
    hPa) indicates the evolution of NO_2 for a calculation with initial O_2 topped up to 1000 hPa .
10   *The plot for $[NO_2]_0 = 344$ hPa additionally shows the increase in NO_2 (thin blue line) at a*
   *temperature rise of 5 K (298 K to 303 K).*
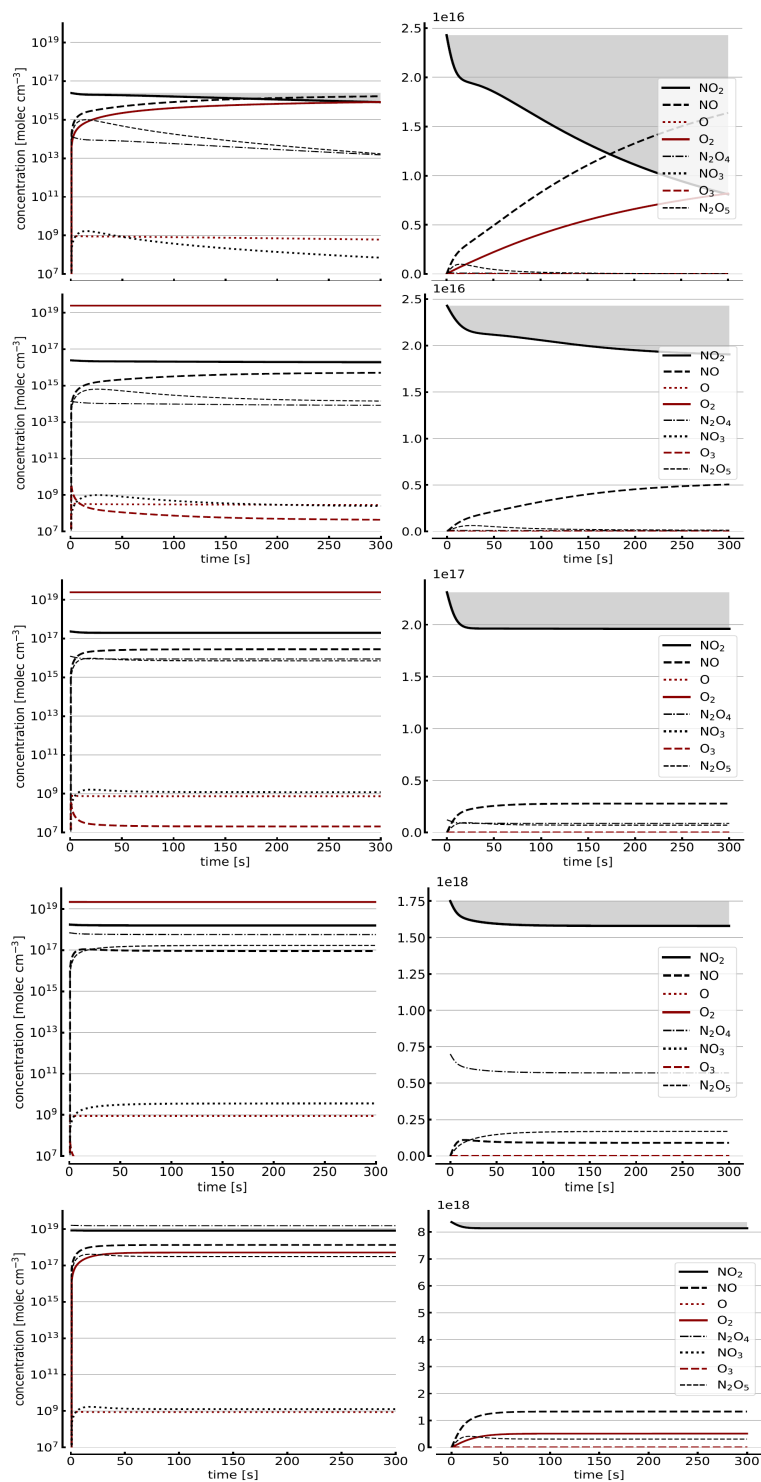
5

Fig. 6: Results of calculations with the full model (reaction 1 to 16, see Table 1). Shown are the temporal evolutions of [NO₂] (thick drawn line), [NO] (dashed line), [O] (dotted line) [O₂] (drawn brown line), [N₂O₄] (dashed-dotted line), [NO₃] (fine dotted line), O₃ (fine dashed line), and [N₂O₅] (thin dashed-dotted line) in an illuminated NO₂-cell. Initial [NO₂]₀ = 1, 1, 10, 71, 344 hPa (2.4·10¹⁶, 2.4·10¹⁷, 1.7·10¹⁸, 0.84·10¹⁹ molec/cm³). Except for the top panel initial O₂ was assumed.
Left panel: logarithmic scale, right panel: linear scale.
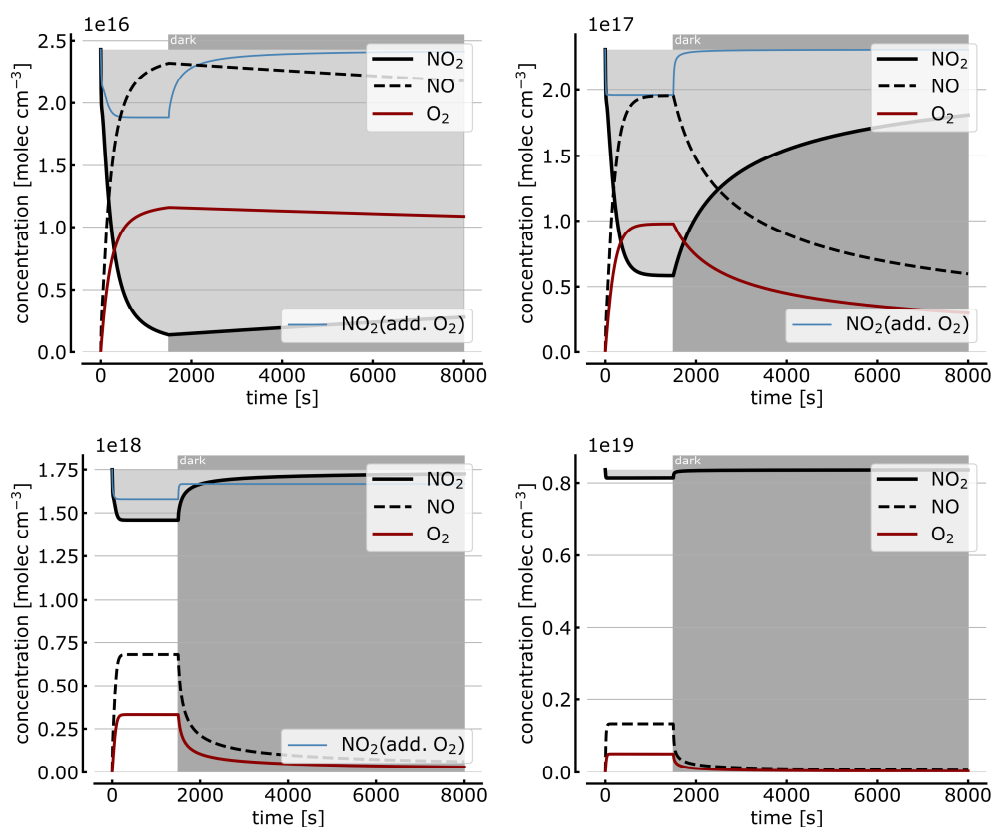
Fig. 7: Recovery of NO₂ in the dark after initial illumination: Model calculations of the temporal evolution of [NO₂] (thick drawn black line), [NO] (dashed black line), [O₂] (drawn brown line) calculated with the full model (reaction 1 to 16, see Table 1, at 298 K). The NO₂-cell is initially illuminated for 1500 s and then left in the dark afterwards. Initial [NO₂]₀ = 1, 1, 10, 71, 344 hPa (2.4·10¹⁶, 2.4·10¹⁷, 1.7·10¹⁸, 0.84·10¹⁹ molec/cm³). The blue thin line in the plots for 1, 10, 71 hPa show [NO₂] for O₂-topped-up cell.

Further calculations encompass the full range of Reaction 1 to Reaction 16 (except wall losses) as given in Table 1, where an analytical solution is not practical or probably even impossible. Figure 6 shows the results of these model runs for NO₂, NO, O-atoms, O₂, N₂O₄, NO₃, O₃, and N₂O₅ in an illuminated NO₂-cell for initial, N₂O₄-equilibrated [NO₂]₀ = 1, 10, 71, 344 hPa (2.4·10¹⁶, 2.4·10¹⁷, 1.7·10¹⁸, 0.84·10¹⁹ molec/cm³). In the top panel no initial O₂ was assumed, the

remaining panels show time series with initial O_2. The left and right panels have logarithmic and linear concentration scales, respectively. Comparison of the result with the data in Figure 5 shows that there are no fundamental differences in the NO_2 time series between the simple model and the full model.

5   As discussed in section 3.1 the recovery of NO_2 in the dark after initial illumination (e.g. due to a use of the cell in a measurement) is an important question. Figure 7 shows model calculations of the temporal evolution of NO_2, NO, and O_2 according to the full model (reaction 1 to 16, see Table 1, at 298 K). The NO_2-cell is initially illuminated for 1500 s and then left in the dark afterwards for initial, N_2O_4-equilibrated $[NO_2]_0 = 1, 10, 71, 344$ hPa ($2.4 \cdot 10^{16}$, $2.4 \cdot 10^{17}$, $1.7 \cdot 10^{18}$,

10   $0.84 \cdot 10^{19}$ molec/cm^3), respectively. At the two highest $[NO_2]_0$ levels the initial NO_2 was chosen such that total pressures of 100 hPa and 1000 hPa, respectively, were reached. It can be seen that the NO_2 recovery at low NO_2 levels can take days to hours. Adding O_2 to the cell again has a strong impact on the $[NO_2]$ evolution (see thin blue lines in Fig. 7), reducing the recovery time to a fraction of the NO_2-only case. For larger initial NO_2 concentrations (e.g. 71 hPa) and added O_2

15   a hysteresis between initial $[NO_2]$ and equilibrium $[NO_2]$ in the dark can be observed, i.e. the NO_2 level does not return to its initial value after illumination. This is due to the formation of N_2O_5 in the illuminated period.

5.   SUMMARY AND CONCLUSIONS

20   We conclude that the use of NO_2 cells requires careful consideration, in particular when quantitative measurements of the NO_2 CD in the cell are desired. If unfortunate parameters are chosen (e.g. rather low NO_2 pressures, no O_2 or air added) practically no NO_2 might be found in the cell at all. Also, one can not say that particularly high or low NO_2 concentrations in the cell are the superior choice. At high NO_2 concentrations (approaching atmospheric pressure) a large

25   fraction of the NO_2 is converted to the dimer N_2O_4, which not only reduces the NO_2 CD way below expected values but also introduces a large temperature dependence (up to 3% per degree) of the NO_2 CD in the cell (also, there might be some uncertainty due to uncertainty of the equilibrium constant as pointed out by Roscoe and Hind, 1993). On the other hand, at low NO_2 levels (e.g. 1 hPa) photolysis may convert much (if not virtually all) of the NO_2 to NO. Although

30   NO_2 eventually recovers, this process may take long (days) to complete. Thus the actual NO_2 CD of the cell may become dependent on the illumination and recovery history of the cell and may be rather unpredictable for a particular cell.

Unfortunately, the two described effects are not even the full story, therefore the potential problems are listed below. Fortunately, there are ways to minimize the problems, like oxygen

35   addition to the cell and choosing the right NO_2 concentration, which may help to reduce the uncertainty of the NO_2 CD of a given cell to the single digit percent range.

5.1. Summary of Problems

As discussed above the NO_2 concentration in a cell - and thus the NO_2 CD of the cell – can deviate from expectations due to a number of reasons:

40

1) Optical effects: multiple reflection in the cell and tilt of the cell with respect to the optical axis can enhance the light path and thus the apparent NO_2 CD
2) Photolysis of NO_2 can reduce the NO_2-CD in the cell
3) Sequestration of NO_2 as N_2O_4 due to the thermodynamic equilibrium between the two

45   species can reduce NO_2 in the cell and cause temperature dependence of the NO_2 CD
4) (re-)formation of NO_2 from NO in the cell leads to slow recovery of NO_2
5) (Irreversible) Conversion of NO_2 to HNO_3 can lead to long-term loss of NO_2
6) Wall loss of NO_X-species like N_2O_4 or N_2O_5 can lead to long-term loss of NO_2

5.2. Some ideas to remedy the situation

One approach to minimize loss of NO_2 in the cell is certainly to reduce the photolysis of NO_2 (R1), this can be achieved by a series of measures:

5
1) Only expose the cell to measurement radiation by e.g. putting it in an nontransparent tube.
2) Minimizing exposure time by e.g. putting the cell in a light-tight box when not in use
3) Use filter in front of the cell which only admits radiation at wavelengths >450 nm, this, however, may interfere with the measurements.

Also, it may be good to avoid ozone photolysis in the cell to minimize OH-formation by using a
10 UV-nontransparent cell material, e.g. glass instead of quartz. In addition it is a good idea to keep the gas in the cell as dry as possible to avoid formation of HNO_3 or HNO_2 and to further minimize OH formation.

A further important measure is to add O_2 to the cell in order to enhance re-conversion of any NO formed to NO_2.

15 The problems associated with excessive N_2O_4 formation in the cell (reduction of the NO_2 CD, temperature dependence of the NO_2 CD, HNO_3 formation) can be reduced by using lower NO_2 concentrations in the cell. The length of the cell may need to be extended to still achieve a desired NO_2 CD. In principle the cell may also be heated to lower the amount of steady state N_2O_4.

20 Problems with the optics of the cell are also difficult to avoid, fortunately they usually lead to changes in the NO_2 CD of <10%. In principle anti-reflective coatings could be used on the cell windows to minimize the problems described in section 2. Another approach would be to tilt the cell with respect to the optical axis thus reflected radiation would not reach the entrance optics of the spectrometer.

25

Acknowledgements:

30

6. LITERATURE

Alicke, B., Platt, U. and Stutz, J.: Impact of nitrous acid photolysis on the total hydroxyl radical budget during the Limitation of Oxidant Production/Pianura Padana Produzione di Ozono study in Milan, J. Geophys. Res., 107, doi: 10.1029/2000JD000075, 2002.

35 Atkinson, R., Baulch, D.L., Cox, R.A., Crowley, J.N., Hampson, R.F., Hynes, R.G., Jenkin, M.E., Ross,i M.J., and Troe, J.: Evaluated kinetic and photochemical data for atmospheric chemistry: Volume I - gas phase reactions of O_x, HO_x, NO_x and SO_x species, Atmos. Chem. Phys., 4(6), 1461-1738, https://doi.org/10.5194/acp-4-1461-2004, 2004.

Bahe, F.C. Marx, W.N., Schurath, U. and Röth, E.P.: Determination of the absolute photolysis rate of
40 ozone by sunlight $O_3+h\nu \rightarrow O(^1D)+O_2(^1\Delta_g)$ at ground level, Atmosph. Environm., 13, 1515-1522; 1979.

Bahe; F. and Schurath; U.: Measurement of $O(^1D)$ Formation by Ozone Photolysis in the Troposphere, Pure and applied Geophys. 116, 537-544, 1978.

Bronstein. I.N., and Semendjajew, K.A.: Taschenbuch der Mathematik, Eds.: G.Grosche and V. Ziegler,
45 19th Edition, Verlag Harri Deutsch, Thun und Frankfurt (Main), 1980.

Burkholder, J.B., Sander, S.P., Abbatt, J., Barker, J.R., Huie, R.E., Kolb, C.E., Kurylo, M.J., Orkin, V.L., Wilmouth, D.M., and Wine, P.H.: Chemical Kinetics and Photochemical Data for Use in Atmospheric

Atmospheric
Measurement
Techniques
Discussions

Studies, Evaluation No. 18, JPL Publication 15-10, Jet Propulsion Laboratory, Pasadena, http://jpldataeval.jpl.nasa.gov, 2015.

Cartry, G., Magne, L., and Cernogora, G.: Atomic oxygen recombination on fused silica: modelling and comparison to low-temperature experiments (300 K), J. Phys. D: Appl. Phys., 33, 1303–1314, 2000.

5   Hönninger, G. and Platt, U.: The Role of BrO and its Vertical Distribution during Surface Ozone Depletion at Alert, Atmos. Environ., 36, 2481-2489, 2002.

Johnston, H.S. and Graham, R.: Photochemistry of NO_x and HNO_x Compounds, Can. J. Chem., 52, 1415-1423, 1974.

Kebabian, P.L., Annen, K.D., Berkoff, T.A., and Freedman, A.: Nitrogen dioxide sensing using a novel gas correlation detector, Meas. Sci. Technol., 11, 499–503, 2010.

Lohberger, F., Hönninger, G., and Platt, U.: Ground Based Imaging Differential Optical Absorption Spectroscopy of Atmospheric Gases, Applied Optics, 43 (24), 4711-4717, 2004.

Lübcke, P., Bobrowski, N., Illing, S., Kern, C., Alvarez Nieves, J.M., Vogel, L., Zielcke, J., Delgado Granados, H., and Platt, U.: On the absolute calibration of SO_2 cameras, Atmos. Meas. Tech., 6 (3), 677–696, doi: 10.5194/amt-6-677-2013, 2013.

Platt, U. and Stutz, J.: Differential Optical Absorption spectroscopy, Principles and Applications, XV, Springer, Heidelberg, 597 pp, 272 illus., 29 in color. (Physics of Earth and Space Environments), ISBN 978-3-540-21193-8, 2008.

Roscoe, H.K. and Hind, A.K.: The equilibrium constant of NO_2 with N_2O_4 and the temperature dependence of the visible spectrum of NO_2: A critical review and the implications for measurements of NO_2 in the polar stratosphere, J. Atmos. Chem., 16, 257, doi: 10.1007/BF00696899, 1993.

Sandsten, J., Edner, H., and Svanberg, S.: Gas imaging by infrared gas-correlation spectrometry, Optics Lett. 21 (23), 1945-1947, 1996.

Sandsten, J., Edner, H., and Svanberg, S.: Gas Visualization of industrial hydrocarbon emissions, Optics Express, 12, 1443, 2004.

Tsang, W. and Hampson, R.F.: Chemical Kinetic Data Base for Combustion Chemistry. Part I. Methane and Related Compounds, J. Phys. Chem. Ref. Data, 15 (3), 1087-1279, 1986.

Trebs, I., Bohn, B., Ammann, C., Rummel, U., Blumthaler, M., Königstedt, R., Meixner, F. X., Fan, S., and Andreae, M.O.: Relationship between the NO_2 photolysis frequency and the solar global irradiance. Atmos. Meas. Tech., 2, 725-739, 2009.

Ward, T.V. and Zwick, H.H.: Gas cell correlation spectrometer: GASPEC, Appl. Optics, 14 (12) 2896-2904, 1975.

35

Appendix 1: Solution of the cubic equation for the stationary state NO concentration:

40   The above Equation 7 is a cubic equation which we recognize as Cardano's formula after substituting z = [NO]:

$$z^3 + pz + q = 0 \tag{22}$$

For which the solution is well known as (e.g. Bronstein and Semendjajew, 1980):

$$z = u + v \tag{23}$$

45   With:

$$u = \sqrt[3]{-\frac{q}{2} + \sqrt{\Delta}}, \quad v = \sqrt[3]{-\frac{q}{2} - \sqrt{\Delta}} \tag{24}$$

And:

$$\Delta = \left(\frac{q}{2}\right)^2 + \left(\frac{p}{3}\right)^3 \tag{25}$$

Equation 7 for z=[NO] thus becomes:

$$[NO]^3 \cdot \frac{k_6}{2J_1} + [NO] - [NO_2]_0 = 0 \tag{26}$$

It is transformed with $a = 2J_1/k_6 \approx 4 \cdot 8 \cdot 10^{-3}/1.95 \cdot 10^{-38} \approx 8.205 \cdot 10^{35}$ molec^2/cm^6 to:

$$[NO]^3 + a[NO] - a[NO_2]_0 = 0 \tag{27}$$

Sample solutions:
1) 1000 hPa of initial NO_2, i.e. $[NO_2]_0 = 2.4 \cdot 10^{19}$:
With $p = a$ and $q = -a[NO_2]_0 \approx -2.4 \cdot 10^{19} \cdot 8.205 \cdot 10^{35} \approx -1.969 \cdot 10^{55}$ and:

$$\Delta = \left(\frac{q}{2}\right)^2 + \left(\frac{p}{3}\right)^3 = \frac{a^2[NO_2]_0^2}{4} + \frac{a^3}{27} \approx 9.694 \cdot 10^{109} + 2.046 \cdot 10^{106} \approx 9.696 \cdot 10^{109} \tag{28}$$

we obtain the only positive and real solution:

$$[NO] = u + v = \sqrt[3]{-\frac{a[NO_2]_0}{2} + \sqrt{\Delta}} + \sqrt[3]{-\frac{a[NO_2]_0}{2} - \sqrt{\Delta}} \tag{29}$$

$$\approx \sqrt[3]{1.969 \cdot 10^{55}} + \sqrt[3]{-2 \cdot 10^{51}} \approx 2.700 \cdot 10^{18} - 1.26 \cdot 10^{17} \approx 2.574 \cdot 10^{18}$$

This means $[NO]/[NO_2]_0$ is about $2.574 \cdot 10^{18}/2.4 \cdot 10^{19} \approx 10.7\%$ of the initial NO_2.

2) At 100 hPa of initial NO_2 ($[NO_2]_0 = 2.4 \cdot 10^{18}$) we obtain $[NO]/[NO_2]_0 \approx 2.4 \cdot 10^{18} \approx 42.9\%$ of the initial NO_2.

3) At 10 hPa of initial NO_2 ($[NO_2]_0 = 2.4 \cdot 10^{17}$) we obtain $[NO]/[NO_2]_0 \approx 2.4 \cdot 10^{17} \approx 94.0\%$ of the initial NO_2.

4) At 1 hPa of initial NO_2, ($[NO_2]_0 = 2.4 \cdot 10^{16}$) we obtain $[NO]/[NO_2]_0 \approx 100\%$ of the initial NO_2.